Molecular Vision 2023; 29:256-265 <http://www.molvis.org/molvis/v29/256>
Received 1 April 2023 | Accepted 1 November 2023 | Published 5 November 2023

Evaluation of the Algerbrush II rotating burr as a tool for inducing ocular surface failure in a mouse model

Athar Shadmani,[1] Trent Jarin,[1] Xiang Qi Meng,[2] Yugendran Rajaendran,[3] Salih Uzun,[1] Albert Y. Wu[1]

[1]Department of Ophthalmology, Stanford University School of Medicine, Stanford, CA; [2]McGill University Faculty of Medicine and Health Sciences, Montreal, Quebec, Canada; [3]Department of Bioengineering, Stanford University School of Engineering and School of Medicine, Stanford, CA

Purpose: The Algerbrush II has been widely used to induce corneal and limbal injuries in animal models. The extent of injury varies with the duration of exposure, pressure from the placement of the burr, and the size of the burr. However, no study has explored the correlation between the duration of exposure and the severity of injury in mouse model with corneal and limbal stem cell deficiency (LSCD) induced using the Algerbrush II. Therefore, this study aimed to evaluate the variations in the severity of corneal and limbal injury with different durations of the Algerbrush II application.
Methods: The entire cornea and limbus of C57BL/6 mice were injured for 30–45 s, 60–75 s, 90–120 s, and 3–4 min. Photography and slit-lamp examination was performed on days 0, 2, 4, and 7, followed by hematoxylin & eosin, periodic acid-Schiff, and immunohistochemical staining. Statistical analysis was performed using one way ANOVA analysis.
Results: A duration of 30–45 s of injury was found to be sufficient to induce superficial corneal and limbal epithelial debridement and re-epithelialization was completed in all eyes by day 7; however, clinical signs of LSCD were not observed in all mice. Increasing the exposure time to 90–120 s resulted in central 2+ corneal opacity with limbal and paracentral corneal neovascularization. All eyes injured for 3–4 min displayed clinical signs of LSCD, such as persistent epithelial defects on day 7 after the injury, central corneal neovascularization, and 2.2+ diffuse corneal opacity. Histological signs of LSCD, including goblet cell metaplasia and K13 expression on the corneal surface, were observed in all injured eyes.
Conclusions: Our findings suggest that the duration of injury is an important factor influencing the severity of LSCD in a murine model of injury. A 1-mm rotating burr was found to be more effective for keratectomy and pigment release, whereas a 0.5-mm burr was more suitable for corneal epithelial debridement.

The cornea is a transparent structure that maintains the eye shape and focuses light on the retina. The cornea can regenerate fully following minor injuries; however, moderate to severe trauma, various immunological reactions, and infections can result in limbal stem cell deficiency (LSCD). This disrupts the barrier function of the limbus, and causes conjunctival epithelial cells to migrate from the conjunctiva to the corneal surface and express cytokeratin K13 instead of K12, which is normally expressed by healthy corneal epithelial cells [1]. K13 is a conjunctival epithelial-specific keratin molecule that is not expressed in the healthy cornea [2]. It is expressed in the injured cornea, which is covered by conjunctival epithelial cells [1].

This condition is called conjunctivalization and manifests as chronic irritation and inflammation, corneal opacity (CO), persistent epithelial defects, and vision loss in severe cases [2-4].

Correspondence to: Albert Y. Wu, Department of Ophthalmology Stanford University School of Medicine 2370 Watson Court, Suite 200 Palo Alto, CA 94303; Phone: (650) 723-6995; FAX: (650) 497-7763; email: awu1@stanford.edu

According to the World Health Organization annual reports in 2001, corneal disease led to vision loss in over 8 million individuals and 1.5 million children [5,6]. Therefore, the development of effective preventive and treatment strategies is critical for addressing the worldwide burden of corneal blindness and disability. Previous studies investigating the pathophysiology of corneal re-epithelialization following corneal and limbal injuries have formed the basis of our understanding of human corneal regeneration after trauma and the efficacy and safety of new regenerative treatments [7-10].

Historically, ocular surface failure models were created using mechanical tools, such as a surgical spatula, Algerbrush II rotating burr, and chemical substances, each resulting in specific outcomes. The selection of an injury model that is appropriate for the aim of the study is an important step that is dependent on several factors, including a deep understanding of the pathophysiology of an injury, as well as the limitations and side effects of each method. For instance, a surgical spatula induces less inflammation; however, it is unsuitable for inducing deep keratectomy, and it induces less stable LSCD in the mouse model [11,12]. Alkali injury is the most favorable choice for inducing ocular surface failure, as it can

be used to induce inflammation and corneal neovascularization (NV) [13]; however, the extent of corneal injury induced is unpredictable, resulting in unwanted complications, such as corneal perforation and auto evisceration [14].

The Algerbrush II rotating burr is an effective and simple tool that is primarily used to remove the rust ring on metal foreign bodies and pannus membranes adhered to the corneal surface. Several previous studies have used the Algerbrush II to induce corneal and limbal injury models [11]. Due to its immense popularity, determining an accurate and reproducible technique that can induce controlled corneal and LSCD in the mouse model is critical. Moreover, it is important for the researcher to familiarize themselves with its complications and limitations as they may interfere with the study results. It is shown that Algerbrush-induced injuries can produce stable CO and LSCD by shaving the limbal epithelium twice, followed by debriding the entire corneal epithelium [12]. Nevertheless, only a limited number of studies have described techniques to induce corneal and LSCD using the Algerbrush II [15], and the required duration of exposure and potential complications remain unclear.

Based on our previous investigations, the severity of corneal and limbal injury induced using the Algerbrush II depends on at least three factors: duration of exposure, pressure applied during surgery, and the size of the burr. This study aimed to investigate the impact of the duration of exposure to the Algerbrush II and the size of the burr on the severity of corneal and limbal injuries while trying to induce a same pressure to all eyes during the procedure.

METHODS

Ethics statement: All procedures were performed in accordance with the Stanford Laboratory Animal Care "APLAC" number 33,420, "Use of Animals for Scientific Purposes," and the "ARVO Statement for the Use of Animals in Ophthalmic and Vision Research." Male and female C57BL/6 mice aged 8–12 weeks were generously provided by the Irving L. Weissman laboratory. The animals were acclimatized to a 12-h light-dark cycle and provided water and feed ad libitum.

Surgical method: Based on the duration of exposure to the Algerbrush II, the animals were divided into four groups of 5 mice in group 1–3 with injury duration of 30–45 s, 60–75 s, 90–120 respectively. Group 4 contained 10 mice with two subgroups with injury duration of 3–4 min. The injury induced in one eye and the other eye was kept as control.

The animals were weighed before inducing intraperitoneal anesthesia which was a mixture of 100 mg/kg of ketamine hydrochloride (ANADA #200–055) and 5 mg/kg of xylazine (NADA #139–236) [16]. The inferior abdominal quadrants were selected as an injection site to avoid potential liver injury [17,18]. Lack of response to toe pinch was indicative of deep anesthesia.

All eyes were examined with a slit-lamp (Nidek SL-450, Nidek Co., Ltd, Aichi, Japan), before surgery to confirm the absence of any previous ocular injuries. The mice were placed in a lateral decubitus position on a surgical table prepared according to standard rodent surgery principles after anesthesia was induced [16]. A pillow measuring 8–10 mm (approximately 0.39 in) in height was placed under the head. Tetracaine hydrochloride (0.5%) eye drops (NDC 0065–0741–12) were administered for further anesthesia. An ophthalmic surgeon (AS) performed the surgery using a Zeiss S5 stereo microscope according to the following procedure. The ocular surface was dried with a surgical eye spear, and the eyelashes were trimmed. The eyelids were gently pressed against the orbital bones to induce proptosis, and the corneal and limbal epithelium was debrided using a sterile Algerbrush II with a 0.5-mm burr (catalog number: SVT14–5-2RB). To equalizing the pressure across the experimental groups the surgical instrument was held gently, and the angle between the burr and corneal surface was maintained at approximately 45° to avoid generating additional pressure. Thus, only the duration of exposure varied among experimental groups.

A timer was used to monitor the duration of Algerbrush II use. The burr was moved in a circular motion beginning at the central part of the cornea, then advanced subsequently to the superior and inferior quadrants without applying any additional pressure.

The duration of injury in group 1 was 30–45 s, and the entire corneal epithelium was debrided while maintaining an intact basement membrane (BM). In group 2, 60–75 s of injury duration was applied, and the corneal and limbal surfaces were shaved twice to remove the corneal and limbus epithelium. The injury duration to the corneal and limbus in group 3 was 90–120 s. To assess the impact of the size of the burr on the extent of injury, we divided group 4 into two groups of five mice. The duration of Algerbrush II use in both groups was 3–4 min; however, a 0.5-mm burr was used in the first subgroup, and a 1-mm burr was used in the second subgroup.

The tip was sanitized with 70% ethylene alcohol before and between surgeries, and the excess debris was cleared from the tip. Any detached epithelial sheets were cleared using a clean eye spear. Care was taken throughout the procedure to avoid damage to the limbal conjunctiva. Tail movement during the surgery was interpreted as a sign of pain

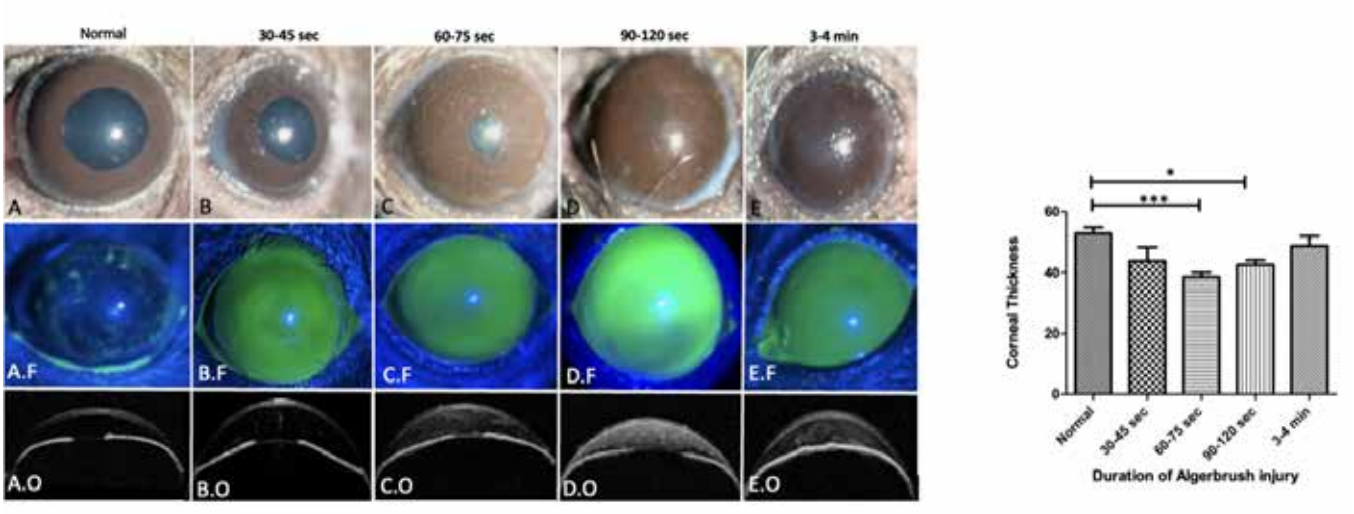

Figure 1. Corneal examination immediately after inducing injury with Algerbrush II. Panels **A**-**E** show typical images of the eyes before (**A**) and following injury (**B**- **E**) when visualized using slit lamp, fluorescent staining (A.F - E.F) and optical coherence tomography (A.O - E.O). **A**: Normal, clear cornea and FS pattern with diffuse punctate epithelial defects and normal OCT with clear anterior chamber, **B**: Following a 30–45 s injury, the cornea is clear with minimal debris in the anterior chamber, **C**: 60–75 s injury results in a mild edema of the cornea with mild release of cells and debris into the anterior chamber that is visible by OCT (C.O), **D**: A 90–120-s injury results in more edema and the release of cells and pigment into the anterior chamber, confirmed with OCT images. **E**: A 3–4 min injury also resulted in significant corneal edema and pigment release. **B**: The corneal thickness in normal eyes and immediately after injury. Statistical analysis revealed significant differences between the normal and 60–75 s and 90–120 s injury duration. However, there was no significant difference between the 3–4 min injured and normal group due to development of corneal edema after prolonged injury. (p value: *=0.0200, ***=0.006).

and addressed by applying a drop of Tetracaine or injecting an additional bolus of 50% of the initial anesthesia volume.

Slit-lamp examination and fluorescent staining (FS) were performed postoperatively. FS was performed by administering 0.1% fluoresceine eye drops (0.1%; diluted from AK-fluor 10%, NDC 17,478-253–10 with buffered saline solution), drying the excess fluorescent liquid, and examining the eye using a cobalt blue filter (Figure 1 and Figure 2).

An ophthalmic ointment containing tetracycline and neomycin was applied postoperatively to prevent wound infection and corneal dryness, and 5 mg/kg of ibuprofen was injected subcutaneously to alleviate post-operative pain. The animals were examined on days 0, 2, 4, and 7.

Clinical evaluation: Slit lamp and Heidelberg Spectralis optical coherence tomography (OCT) examinations were performed to evaluate the cornea and anterior chamber on days 0, 2, 4, and 7 after the surgery. The animals were anesthetized before the examination, as described previously. Photographs were captured using the iPhone 13 camera in Cinematic mode. ImageJ was used on the fluorescent-stained images to calculate the ratio of epithelial defects (ED) to the entire corneal surface.

CO was scored on a scale of 1 to 4 based on the classification by Yoeruek et al. [19]: 0=normal, clear; 1=mild opacity; 2=severe opacity, but the iris and pupil are easily distinguishable; 3=iris and pupil are barely distinguishable; and 4=completely opaque with an invisible pupil.

The corneal NV was graded in accordance with the method by Bahar et al. with modifications [20]. Limbal NV was restricted to the limbus, paracentral NV extended from the limbus to the periphery of the cornea, and central NV extended to the pupillary area within 1 mm of the central cornea.

Scoring system of the OCT images: Two different anterior OCT images were selected for each eye. The corneal thickness was measured in pixels at three separate locations in each image, the values were converted to micrometers, and the average and standard deviation for each group were calculated and compared with those of other groups.

Histologic evaluation: Enucleation was performed after euthanizing the animals. Histological evaluation was performed on postoperative days 4 and 7. The enucleated eyes were fixed in 10% formalin overnight at room temperature, dehydrated using a series of graded alcohols and xylene, and subsequently encased in paraffin. The paraffin blocks were cut into 6-µm-thick sections and mounted on glass microscope slides. Hematoxylin and eosin (H&E) and periodic acid-Schiff (PAS) staining were performed. All layers of the cornea and anterior

chamber were evaluated, and the severity of inflammation was assessed for each group. The remaining sections were subsequently used for immunostaining. The slides were deparaffinized using xylene and graded alcohol. Epitope retrieval (ER) was performed before immunostaining by immersing the deparaffinized slides in Citrate Buffer with pH 6.0 for 20 min at 85 °C. The slides were immersed for another 20 min at room temperature to cool down, then reheated as described previously. After rinsing in staining buffer (10 mM Tris buffered saline with 0.025% Triton X-100), antigen blocking was performed for one hour using BSA (BSA) 5%. The slides were incubated in a buffer containing primary keratin 13 antibodies (K13; a 1:100 dilution of mouse monoclonal, Cat. No. ab92551, Abcam, Cambridge, UK) overnight at 4 °C. Donkey anti-Mouse-IgG (A10037) at a dilution of 1:500 was used to detect the binding of the primary antibodies. Negative controls were created by circumventing the primary antibody incubation step. Positive controls consisted of non-wounded tissue sections stained with keratin 13 antibodies. The slides were imaged using a Leica Thunder Imager microscope.

Statistical analysis: Statistical analysis comparing multiple groups with parametric data was performed by one way ANOVA (GraphPad Prism) analysis. All data were presented as mean ± standard deviation. The Tukey's multiple comparison test was used for additional subgroup analysis. A value of $p<0.05$ was considered statistically significant.

RESULTS

Slit lamp examination findings: Table 1 summarizes the main findings of the study. Corneal edema and exudation release into the anterior chamber, immediately after injury induction,

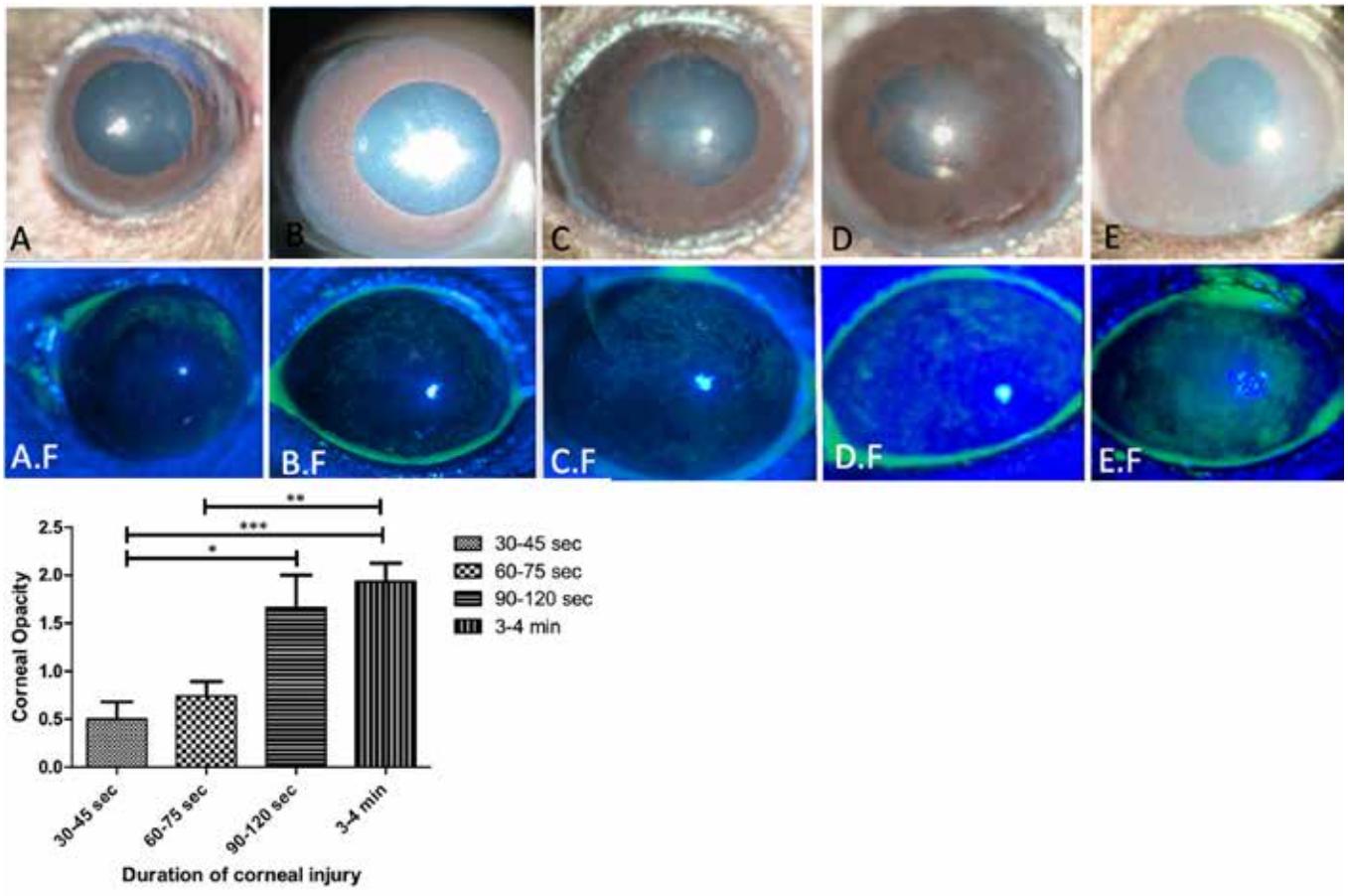

Figure 2. The eyes 7 days after the injury using slit lamp, 2A- **A**: 30–45 s, **B**: 60–75 s, **C**: 90–120 s, **D**: 90–120 s, E: 3–4 min. **A** and **B**: The cornea is almost completely recovered with normal diffuse punctate epithelial defects. **C** and **D**: A 90–120-s injury, results in 2+ corneal opacity with centrally distributed new vessel formation and pigment deposition on the endothelial layer. **E**: A 3–4 min injury results in diffuse CO with a large epithelial defect. **B**: The density of corneal opacity increased with the duration of the injury. CO in all groups were compared by Tukey's Multiple Comparison Test. Statistically significant difference is observed between groups 30–45 s, 60–120 s and 3–4 min injury groups. * p value=0.001 *** p value=0.0009.

were minimal in group 1. However, exudate release was observed after around 60 s of injury and was significantly increased on advancing the exposure time to 2 min and more. Group four has the most severe exudate release compared to other groups (Figure 1).

During the first week post injury in group 1 and 2, re-epithelialization occurred, and edema decreased continuously from the peripheral to the central cornea. In group 3, 75% of eyes were completely re-epithelialized with negative FS, which was a clinical sign of basement membrane disease [21]. In group 4, none of eyes were completely re-epithelialized after 7 days of injury and the mean epithelial defect was 50.38%.

On day 7, the mean CO in group 1 was 0.5+ and 25% developed corneal NV. The mean CO in group 2 was 0.8+ and 33% of eyes developed corneal NV. The mean score of CO in group 3 and 4 were 2+ and 2.2+ respectively which was diffusely distributed to the cornea. 100% of the eyes showed corneal NV in both groups. A statistically significant difference in CO was observed between group 1, group 3, and 4 (Figure 2).

Regarding the tip size of Algerbrush, the mean CO induced by the 1-mm and 0.5-mm burrs were 2.33 and 1.9, respectively, which was statistically significant (p value=0.029).

OCT findings: The corneal thickness was measured in all groups after injury induction. Statistical analysis revealed significant differences between the normal and 60–75 s and 90–120 s injury duration (Figure 1B). However, there was no significant difference between normal corneal and the 3–4 min injured cornea due to development of corneal edema after prolonged injury (Figure 3).

Histology and immunohistology findings: The H&E-stained corneal section of the C57BL/6 mice were observed under the light microscope with 40X magnification is shown in Figure 4A,B. The epithelium, which comprised 4–5 cell layers and BM, covered the corneal stroma.

Immediately after the injury, the corneal epithelium was eliminated and the cornea exhibited an irregular stromal surface. The iris vessels were dilated and the anterior chamber was filled with exudate (Figure 4C,D). On day 4 after the injury, the conjunctival epithelial cell layers proliferated, with prominent nuclei migrating through the limbus to the central corneal area (Figure 5A).

On day 7 after the injury, the corneal surface was covered with a thin and atrophic layer of epithelial cells in all groups except the eyes in group 4, which still exhibited stroma with central denudation. The endothelium was reactive and covered with pigments and exudate.

Table 1. Main study findings 7 days after injury, n=5

Tme	CO	NV	FS
	Mean-location percentage	Location percentage	Pattern
30–45 s	0.5-C-50%	L-25%	Diffuse punctate ED
60–75 s	0.8-C and D-80%	PC-33%	Diffuse punctate and patchy
90–120 s	2-C and D-100%	PC-100%	Diffuse punctate and patchy ED
3–4 min	2.2-D-100%	PC-100%	Patchy ED 50.38%

The mean corneal opacity (CO), neovascularization (NV), and fluorescent staining (FS) and their location and the percentage of eyes that developed corneal opacity and neovascularization on day 7 after the injury. Prolonged injury induction for 90–120 s and more induced CO in all eyes, but light injuries to the cornea and limbus did not result in CO in all injured eyes. The average epithelial defect was 50.38% of the corneal surface 7 days after 3–4-min of injury induction. C: central, D: diffuse, PC: paracentral, L: limbal, ED: epithelial defect

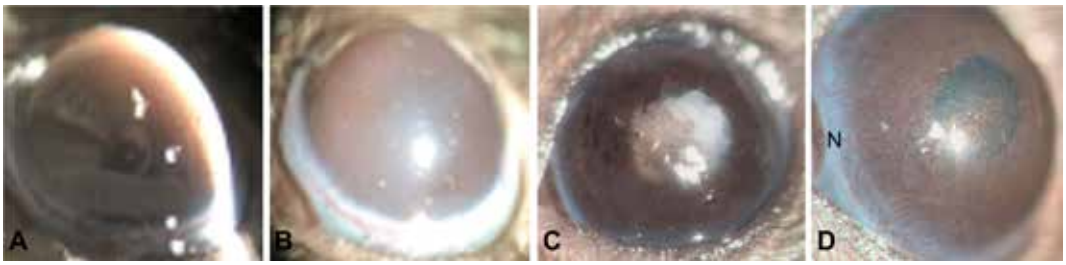

Figure 3. Complications of Algerbrush injury. Intense exudate and pigment in the anterior chamber accompanied by corneal edema immediately after a 3–4 min injury (**A** and **B**). **C**: Cataract with pigment deposition on the endothelial layer is seen one week after injury induction. **D**: Formation of new vessel in the cornea that extends to the center of the cornea one week after a 2-min injury. N: nasal side of the eye.

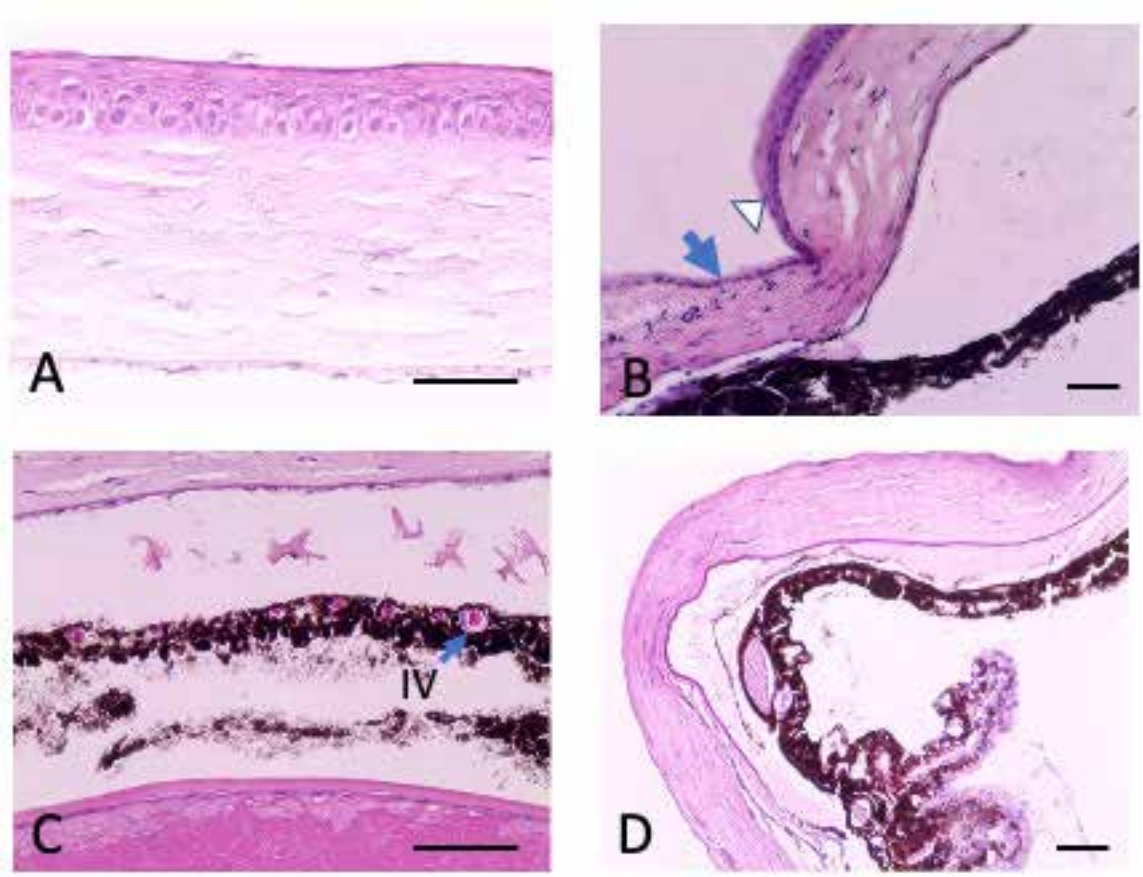

Figure 4. Hematoxylin and eosin-stained mouse corneal section visualized under bright light. **A**: Normal corneal epithelial cells attach to the basement membrane. Corneal spindle shaped keratocytes are distributed throughout the stromal layer and normal endothelial cells cover the descemet membrane. **B**: The limbus is a transitional zone where conjunctival epithelial cells transform from monolayered conjunctival epithelial cells (blue arrow) to multi-layered corneal epithelial cells in the cornea (white arrowhead). The normal anterior chamber (AC) is clear with no exudate or cells. The normal iris is thin with constricted blood vessels. **C**: Dilated iris vessels (IV) and exudate deposition on the endothelial layer are illustrated. Longer durations of injury result in more pigment release into the anterior chamber. **D**: immediately after Algerbrush injury, the corneal and limbal epithelial cells are absent. [40X and 20X Magnification under an EVOS XL Core microscope, Scale bar=50 µm]..

Figure 5. Mouse corneal epithelium on days 4 (**A**) and 7 (**B** and **C**) after Algerbrush II injury. **A**: Multiple layers of regenerated conjunctival epithelial cells have accumulated at the limbal region moving toward the corneal center. **B**: The limbal epithelium has returned to its normal monocellular layer state 7 days after injury induction (arrowhead). **C**: The corneal surface is covered by an atrophic monolayer of basal epithelial cells with goblet cells scattered throughout the surface. Scale bar=50 µm.

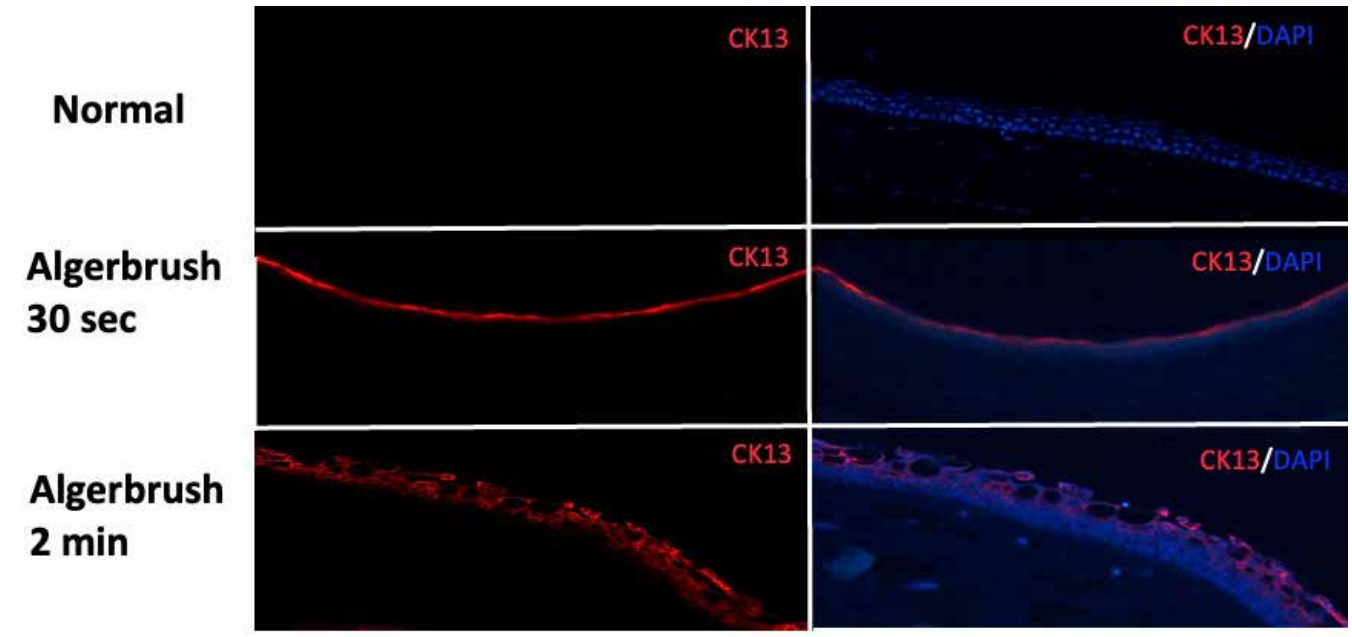

Figure 6. Identification of conjunctivalization using immunofluorescence. Conjunctival epithelial phenotype (K13) is sparsely visible in the normal corneal specimen. However, the K13 marker identified in the injured cornea on day 7 confirmed corneal conjunctivalization even in mild, 30-s corneal injury (Algerbrush 30 s). The density of K13 has increased after increasing the duration of injury to 2 min (Algerbrush 2 min).

Goblet cells were detected on the corneal surface in the PAS-stained slides in all groups which was a marker of conjunctivalization (Figure 5B,C). The immunohistochemical staining, revealed the expression of K13 on the corneal surface which were expressed from the epithelial cells with conjunctival origin that covered the injured cornea and confirmed conjunctivalization (Figure 6).

3.4 Complications of Algerbrush II injury: The vibrations from the Algerbrush II burr transferred to the eyeball and likely resulted in pigment release from the ciliary body and iris into the anterior chamber, especially in groups that were exposed for more than 2 min (Figures 3). Another complication included bleeding from the conjunctival or limbal vessels, which was avoided by applying gentle pressure on the limbus using the Algerbrush II. Furthermore, cataracts and iris neovascularization were detected in the eyes with prolonged exposure to the Algerbrush II (Figure 3C).

DISCUSSION

Animal models play a vital role in the development of therapies for the treatment of corneal disorders. A reliable initial injury model that is tailored for the purpose of the study is a prerequisite for the evaluation of the effectiveness of different preventive and therapeutic modalities. Due to the immense popularity of the Algerbrush II, this study investigated the effects of this device on the creation of LSCD models to provide additional insight and guidance for researchers.

Ocular surface failure occurs due to a deficiency of the epithelial progenitor cells that are required to maintain the corneal epithelium. In humans, the progenitor cells are concentrated within epithelial crypts which are located in a narrow transitional zone of tissue known as the corneal limbus [22]. However, unlike the human cornea, the distribution of stem cells in the murine cornea is not limited to the limbus, and the limbus is not the only niche for corneal stem cells. The cornea is self-maintained and contains corneal epithelial stem cells distributed in the basal layer of the entire cornea and limbus in some mammals [23,24]. Therefore, superficial debridement of the limbus or cornea does not destroy all stem cell niches distributed throughout the cornea.

Corneal and LSCD result in clinical and histological changes. The clinical signs include CO, persistent epithelial defects, and diffuse corneal NV [3,25]. The histological signs are based on the presence of conjunctival epithelial cells on the corneal surface, such as goblet cell metaplasia and K13 expression.

Goblet cells are mucin-producing cells that are distributed throughout the conjunctival epithelial cells but not on the corneal surface [25,26]. After limbal injury goblet cells arising from conjunctival epithelial cell metaplasia, appear

on the corneal surface. This is an important sign of conjunctivalization and LSCD [27,28].

Our findings suggest that 30–45 s of corneal injury can induce incomplete progenitor cells destruction that results in the appearance of goblet cells and K13 expression on the corneal surface histologically. However, clinical signs of LSCD, such as diffused CO and corneal NV, were not visible in the majority of injured eyes. This finding can be attributed to the remanent corneal and limbal stem cell reservoirs that adequately repopulate the corneal surface and maintain corneal clarity, with additional partial contribution of the conjunctival cells. Increasing the duration of injury to 2 min and more resulted in more severe destruction of the corneal and limbal stem cell niches that result in both clinical and histological manifestation of LSCD.

Another finding of our study was that, similar to human eyes, the nasal part of the mouse cornea is more susceptible to new vessel formation compared with the temporal part [30]. This may be due to the fewer sub-basal nerves at the nasal cornea compared to the central and temporal parts [31,32]. The sub-basal sensory nerve fiber layer plays a crucial role in continuously releasing neuropeptides and other growth-promoting substances, which are necessary for providing essential nutrients to support the differentiation and growth of corneal epithelial cells [33]. As a result, areas with fewer sub-basal nerve endings experience a delay in the regeneration of the corneal epithelium compared to areas with a higher density of nerve endings. Consequently, the slowed regeneration of the corneal epithelium following an injury can lead to an elevated secretion of VEGF, thereby promoting the development of corneal NV on the surface of the cornea. Further studies in this direction are required in the future to gain insight into this issue.

According to our study, the 1-mm burr is more suitable for keratectomy, pigment, and exudate release, whereas the 0.5-mm burr is more suitable for epithelial debridement with preservation of the BM.

As with all techniques, researchers must consider several additional variables that may influence the outcome. An even movement of the burr over the cornea, the function and maintenance of the equipment, the age and strain of the animal are important variables that must be considered to obtain an accurate result.

Due to the development of progressive corneal edema during prolonged injury, prediction of the depth and thickness of the removed cornea is difficult in this model. Therefore, an excimer laser or adjustable diamond knife may be considered in studies requiring the removal of a precise depth of corneal tissue.

In conclusion, the present study is the first to demonstrate that the duration of Algerbrush injury plays an important role in the creation of a murine model of corneal and LSCD with histological and clinical signs of LSCD. Debridement of the corneal epithelium can be performed in 30–45 s, whereas inducing LSCD and diffuse CO require at least 2 min of injury induction. A 3–4 min exposure produces diffuse CO and persistent epithelial defect with centrally distributed NV. Our findings provide additional insight into creating a reproducible corneal and LSCD model to help gain insight into the wound healing process and preclinical studies.

ACKNOWLEDGMENTS

We acknowledge that NEI P30EY026877 and Research to Prevent Blindness grants supported this research. We thank Dr. Ian James Dryden for helping and guiding the interpretation of the histology slides. We thank Charlene Wang, Dr. Irving Weissman, and his laboratory at Stanford University's Institute for Stem Cell Biology and Regenerative Medicine for their kind assistance in providing the animals. We also sincerely thank Aditi Swarup, Hala Shakib Dhowre, and Abbie Kiok Maemoto for their guidance and help with the imaging techniques. None of the researchers have a financial interest in any of the companies or products described in this study.

REFERENCES

1. Kao WWY. Keratin expression by corneal and limbal stem cells during development. Exp Eye Res 2020; 200:108206[PMID: 32882212].

2. Danjo S, Friend J, Thoft RA. Conjunctival epithelium in healing of corneal epithelial wounds. Invest Ophthalmol Vis Sci 1987; 28:1445-9. [PMID: 3623830].

3. Deng SX, Borderie V, Chan CC, Dana R, Figueiredo FC, Gomes JAP, Pellegrini G, Shimmura S, Kruse FE. and The International Limbal Stem Cell Deficiency Working Group. Global consensus on the definition, classification, diagnosis and staging of limbal stem cell deficiency. Cornea 2019; 38:364-75. [PMID: 30614902].

4. Chen JJ, Tseng SC. Abnormal corneal epithelial wound healing in partial-thickness removal of limbal epithelium. Invest Ophthalmol Vis Sci 1991; 32:2219-33. [PMID: 1712763].

5. Whitcher JP, Srinivasan M, Upadhyay MP. Corneal blindness: a global perspective. Bull World Health Organ 2001; 79:214-21. [PMID: 11285665].

6. Ament JD, Todani A, Pineda R 2nd, Shen TT, Aldave AJ, Dohlman CH, Chodosh J. Global corneal blindness and the

Boston keratoprosthesis type I. Am J Ophthalmol 2010; 149:537-9. [PMID: 20346774].

7. Tang Q, Lu B, He J, Chen X, Fu Q, Han H, Luo C, Yin H, Qin Z, Lyu D, Zhang L, Zhou M, Yao K. Exosomes-loaded thermosensitive hydrogels for corneal epithelium and stroma regeneration. Biomaterials 2022; 280:121320[PMID: 34923312].

8. Shojaati G, Khandaker I, Funderburgh ML, Mann MM, Basu R, Stolz DB, Geary ML, Dos Santos A, Deng SX, Funderburgh JL. Mesenchymal Stem Cells Reduce Corneal Fibrosis and Inflammation via Extracellular Vesicle-Mediated Delivery of miRNA. Stem Cells Transl Med 2019; 8:1192-201. [PMID: 31290598].

9. Holan V, Trosan P, Cejka C, Javorkova E, Zajicova A, Hermankova B, Chudickova M, Cejkova J. A comparative study of the therapeutic potential of mesenchymal stem cells and limbal epithelial stem cells for ocular surface reconstruction. Stem Cells Transl Med 2015; 4:1052-63. [PMID: 26185258].

10. Antunes-Foschini R, Adriano L, Murashima AAB, Barbosa AP, Nominato LF, Dias LC, Fantucci MZ, Garcia DM, Alves M, Rocha EM. Limitations and advances in new treatments and future perspectives of corneal blindness. ABO 2021; 84.

11. Stepp MA, Zieske JD, Trinkaus-Randall V, Kyne BM, Pal-Ghosh S, Tadvalkar G, Pajoohesh-Ganji A. Wounding the cornea to learn how it heals. Exp Eye Res 2014; 121:178-93. [PMID: 24607489].

12. Afsharkhamseh N, Movahedan A, Gidfar S, Huvard M, Wasielewski L, Milani BY, Eslani M, Djalilian AR. Stability of limbal stem cell deficiency after mechanical and thermal injuries in mice. Exp Eye Res 2016; 145:88-92. [PMID: 26607808].

13. Bai JQ, Qin HF, Zhao SH. Research on mouse model of grade II corneal alkali burn. Int J Ophthalmol 2016; 9:487-90. [PMID: 27162717].

14. Shadmani A, Razmkhah M, Jalalpoor MH, Lari SY, Eghtedari M. Autologous Activated Omental versus Allogeneic Adipose Tissue-Derived Mesenchymal Stem Cells in Corneal Alkaline Injury: An Experimental Study. J Curr Ophthalmol 2021; 33:136-42. [PMID: 34409223].

15. 15. Shah D, Aakalu VK. Murine Corneal Epithelial Wound Modeling. In: Das H, ed. *Wound Regeneration: Methods and Protocols*. Methods in Molecular Biology. Springer US; 2021:175–181.

16. Hoogstraten-Miller SL, Brown PA. Techniques in Aseptic Rodent Surgery. Curr Protoc Immunol 2008; 82:1-.

17. Field K, Bailey M, Foresman LL, Harris RL, Motzel SL, Rockar RA, Ruble G, Suckow MA. Medical records for animals used in research, teaching, and testing: public statement from the American College of Laboratory Animal Medicine. ILAR J 2007; 48:37-41. [PMID: 17170494].

18. Bogdanske JJ, Hubbard-Van Stelle S, Riley MR, Schiffman B. *Laboratory Mouse Procedural Techniques: Manual and DVD*. CRC Press; 2010.

19. Yoeruek E, Ziemssen F, Henke-Fahle S, Tatar O, Tura A, Grisanti S, Bartz-Schmidt KU, Szurman P. Tübingen Bevacizumab Study Group. Safety, penetration and efficacy of topically applied bevacizumab: evaluation of eyedrops in corneal neovascularization after chemical burn. Acta Ophthalmol 2008; 86:322-8. [PMID: 17995975].

20. Bahar I, Kaiserman I, McAllum P, Rootman D, Slomovic A. Subconjunctival bevacizumab injection for corneal neovascularization. Cornea 2008; 27:142-7. [PMID: 18216566].

21. Korkmaz I, Barut Selver O, Simsek C, Palamar M. Negative Corneal Fluorescein Staining as an Exceptionally Early Sign of Acanthamoeba Keratitis: A Case Report. Eye Contact Lens 2021; 47:622-4. [PMID: 34348354].

22. Schermer A, Galvin S, Sun TT. Differentiation-related expression of a major 64K corneal keratin in vivo and in culture suggests limbal location of corneal epithelial stem cells. J Cell Biol 1986; 103:49-62. [PMID: 2424919].

23. Li J, Xiao Y, Coursey TG, Chen X, Deng R, Lu F, Pflugfelder SC, Li DQ. Identification for Differential Localization of Putative Corneal Epithelial Stem Cells in Mouse and Human. Sci Rep 2017; 7:5169-[PMID: 28701781].

24. Majo F, Rochat A, Nicolas M, Jaoudé GA, Barrandon Y. Oligopotent stem cells are distributed throughout the mammalian ocular surface. Nature 2008; 456:250-4. [PMID: 18830243].

25. Tseng SC, Hirst LW, Farazdaghi M, Green WR. Goblet cell density and vascularization during conjunctival transdifferentiation. Invest Ophthalmol Vis Sci 1984; 25:1168-76. [PMID: 6207137].

26. Rivas L, Oroza MA, Perez-Esteban A, Murube-del-Castillo J. Topographical distribution of ocular surface cells by the use of impression cytology. Acta Ophthalmol (Copenh) 1991; 69:371-6. [PMID: 1927322].

27. Shapiro MS, Friend J, Thoft RA. Corneal re-epithelialization from the conjunctiva. Invest Ophthalmol Vis Sci 1981; 21:135-42. [PMID: 7251297].

28. Park M, Zhang R, Pandzic E, Sun M, Coulson-Thomas VJ, Di Girolamo N. Plasticity of ocular surface epithelia: Using a murine model of limbal stem cell deficiency to delineate metaplasia and transdifferentiation. Stem Cell Reports 2022; 17:2451-66. [PMID: 36270283].

29. Wei ZG, Wu RL, Lavker RM, Sun TT. In vitro growth and differentiation of rabbit bulbar, fornix, and palpebral conjunctival epithelia. Implications on conjunctival epithelial transdifferentiation and stem cells. Invest Ophthalmol Vis Sci 1993; 34:1814-28. [PMID: 8473120].

30. Alqahtani JM. The prevalence of pterygium in Alkhobar: A hospital-based study. J Family Community Med 2013; 20:159-61. [PMID: 24672272].

31. He J, Bazan HE. Neuroanatomy and Neurochemistry of Mouse Cornea. Invest Ophthalmol Vis Sci 2016; 57:664-74. [PMID: 26906155].

32. McKenna CC, Lwigale PY. Innervation of the mouse cornea during development. Invest Ophthalmol Vis Sci 2011; 52:30-5. [PMID: 20811061].

33. Stepp MA, Tadvalkar G, Hakh R, Pal-Ghosh S. Corneal epithelial cells function as surrogate Schwann cells for their sensory nerves. Glia 2017; 65:851-63. [PMID: 27878997].

Articles are provided courtesy of Emory University and the Zhongshan Ophthalmic Center, Sun Yat-sen University, P.R. China. The print version of this article was created on 5 November 2023. This reflects all typographical corrections and errata to the article through that date. Details of any changes may be found in the online version of the article.